decay (T_1) processes due to radiative or nonradiative decay or excitation trapping play no significant role in dephasing since $T_1 = 5$ msec at 2 K corresponding to linewidth of 32 Hz.

In conclusion we have observed coherent transients in a stoichiometric material for the first time and find qualitatively new behavior, i.e., a substantial variation of T_2 across the inhomogeneously broadened line. These photon-echo measurements on EuP_5O_{14} are interpreted as evidence for delocalization of the Eu^{3+} excitation. The surprisingly long dephasing times observed ($T_2 \sim 20$ μsec) should stimulate further application of powerful optical coherent transient techniques to the study of coherence in excitonic systems.

The EuP_5O_{14} crystals used in this experiment had been grown by Dr. F. Lutz of the University of Hamburg and kindly supplied by Dr. G. Huber and Professor H. Danielmeyer. The authors wish also to thank M. J. Weber for a crystal of $YAlO_3:Eu^{3+}$ and acknowledge stimulating discussions with A. Z. Genack and M. D. Levenson. This work was supported in part by the Air Force Office of Scientific Research under Contract No. F49620-79-C-0108.

[1]R. L. Shoemaker, Ann. Rev. Phys. Chem. 30, 239 (1979).
[2]H. G. Danielmeyer and H. P. Weber, IEEE J. Quantum Electron. 8, 805 (1972).
[3]R. M. Macfarlane, R. M. Shelby, and R. L. Shoemaker, Phys. Rev. Lett. 43, 1726 (1979).
[4]H. Y.-P. Hong, Acta Crystallogr., Sect. B 30, 468 (1974).
[5]C. Brecher, J. Chem. Phys. 61, 2297 (1974).
[6]R. G. DeVoe, A. Szabo, S. C. Rand, and R. G. Brewer, Phys. Rev. Lett. 42, 1560 (1979).
[7]R. J. Elliott, Proc. Phys. Soc. London, Sect. B 70, 119 (1957).
[8]I. D. Abella, N. A. Kurnit, and S. R. Hartmann, Phys. Rev. 141, 39 (1966).
[9]K. Krebs and R. Winkler, Naturwissenschaften 47, 490 (1960).
[10]R. M. Macfarlane, R. M. Shelby, A. Z. Genack, and D. A. Weitz, to be published.
[11]J. Koo, L. R. Walker, and S. Geshwind, Phys. Rev. Lett. 35, 1669 (1975).
[12]P. Avouris, A. Campion, and M. A. El-Sayed, J. Chem. Phys. 67, 3397 (1977).
[13]P. M. Selzer, D. L. Huber, D. S. Hamilton, W. M. Yen, and M. J. Weber, Phys. Rev. Lett. 36, 813 (1976).
[14]T. Holstein, S. K. Lyo, and R. Orbach, Phys. Rev. B 15, 4693 (1977).
[15]R. Flach, D. S. Hamilton, P. M. Selzer, and W. M. Yen, Phys. Rev. B 15, 1248 (1977).

Measurements of the Beam-Driven Current in the DITE Tokamak

W. H. M. Clark, J. G. Cordey, M. Cox, R. D. Gill, J. Hugill, J. W. M. Paul, and D. F. H. Start
EURATOM–United Kingdom Atomic Energy Authority Fusion Association, Culham Laboratory, Abingdon, Oxon OX14 3DB, United Kingdom
(Received 12 May 1980)

The beam-driven current produced by neutral injection into the DITE tokamak has been measured. The variation of this current with electron density and gas current has also been investigated. Good agreement is found between experiment and a model in which the Fokker-Planck equation describes the fast-ion distribution and a magnetic field diffusion equation gives the time dependence of the electromagnetic fields.

PACS numbers: 52.40.Mj, 52.55.Gb

The possibility of using fast ions produced by tangential neutral injection to generate a current in a toroidal reactor was first proposed by Ohkawa.[1] This beam-driven current has been observed in the Culham Laboratory Levitron.[2] Here we report the first measurements of this current in a tokamak.

The experiments were performed on the DITE tokamak[3] which has major and minor radii $R = 1.17$ m and $a = 0.26$ m, toroidal field $B_T \leq 2.7$ T and plasma current $I_p \leq 250$ kA. The neutral-hydrogen injection system[4] provides power $P_I \leq 1.2$ MW to the plasma at energies up to 24 keV, with the beam in a tangential direction.

In DITE the beam-driven current changes the plasma loop voltage because the Ohmic-heating transformer circuit maintains the total current approximately constant. When the beam is in the same direction (coinjection) as the transformer induced current, some of the latter is replaced by the beam-driven current and the required loop voltage (V_l) is reduced. For counterinjection

the opposite occurs. However, V_l can also be affected by changes in electron temperature profile $T_e(r)$ and the plasma effective ionic charge ($Z_{\rm eff}$). These quantities were, therefore, measured and their effect on V_l calculated. The reduction in $Z_{\rm eff}$ caused by charge exchange of the beam with the impurity species[5] is negligible and the reduction caused by injection of particles with atomic number $Z_b = 1$ is small and is neglected. [For example, the dilution of the low-density He discharge *A* (Table I) could reduce $Z_{\rm eff}$, and hence V_l, by a maximum of 10% after 10 ms of injection compared with the observed 50% change in V_l.]

The magnitude of the beam-driven current depends upon the circulating fast ion current. This exceeds the equivalent injected current by the stacking factor $S = v_f \tau_s / 2\pi R$ where v_f is the fast ion velocity and the slowing down time τ_s varies as $T_e^{3/2}/n_e$, where n_e is the electron density. Thus S is greatest for low n_e and high T_e. However, at low n_e the plasma neutral density is larger and an appreciable fraction of the fast ions can be lost by charge exchange. Because the charge-exchange cross section is lower for He, most of the experiments used helium target plasmas.

Experiments were conducted over a range of electron densities and gas currents for both D and He plasmas (Table I). The plasma loop voltage (Fig. 1) showed a substantial drop during injection. The profiles of T_e (Fig. 2) from Thomson scattering and n_e from 2-mm–microwave interferometry were measured before, during, and after injection. The profiles taken before and after injection are used to calculate $Z_{\rm eff}$. During injection $Z_{\rm eff}$ cannot be measured by this method because of the effect of the beam-driven current. A linear variation of $Z_{\rm eff}$ with time during injection is assumed. For several of the discharges of Table I this is supported by x-ray anomaly factor (defined in Ref. 6) measurements.

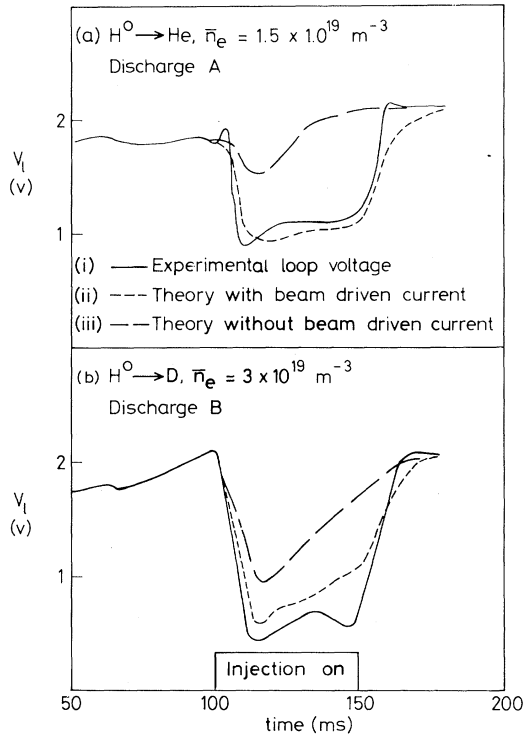

FIG. 1. Experimental and calculated plasma loop voltages.

These show that for discharge *C*, for example, the change in V_l caused by impurity concentration changes is $\leq \pm 0.3$ V.

The measurements of V_l are compared with a theoretical model similar to that used by Singer *et al.*[7] However, the experimental profiles of n_e and T_e are used as input to the model instead of theoretical profiles. The fast ion current is obtained from the Fokker-Planck drift kinetic equation which includes fast ion collisions with the thermal ions and electrons, and acceleration of the fast ions by the electric field. The equation is solved numerically as a function of time on

TABLE I. Summary of experimental results before (first value) and during (second value) injection for each discharge.

Discharge, working gas	I_p (kA)	B_T (T)	V_l (V)	$n_e(0)$ (10^{19} m^{-3})	$T_e(0)$ (keV)	$Z_{\rm eff}$	P_I (MW)
(*A*), He	80, 80	2.2	1.8, 1.1	2.2, 4.0	0.58, 0.67	3.0, 4.0	0.9
(*B*), D_2	90, 95	2.2	2.1, 0.4	3.0, 5.0	0.63, 0.90	1.9, 2.8	1.0
(*C*), He	92, 94	2.2	1.9, 1.1	1.6, 3.1	0.65, 0.67	3.7, 3.7	0.95
(*D*), He	94, 94	2.2	2.0, 1.2	6.2, 7.8	0.63, 0.69	1.7, 2.1	0.95
(*E*), He	167, 167	2.7	1.5, 1.2	2.5, 5.0	1.4, 1.1	3.0, 5.0	0.97
(*F*), He	−156, −156	2.7	−1.4, −2.2	2.8, 4.1	0.91, 0.74	1.9, 3.0	1.0

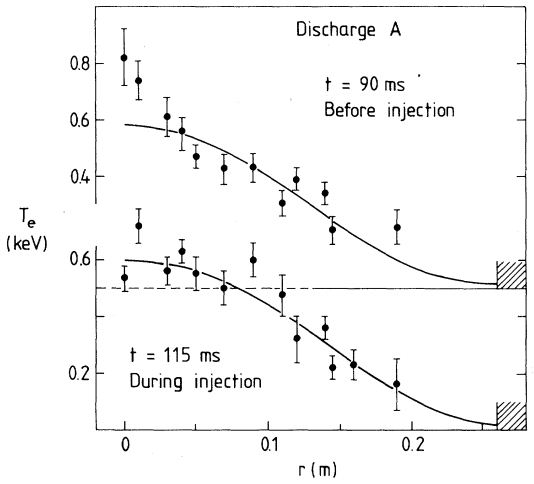

FIG. 2. Profiles $T_e(r)$. The solid lines are best fits of an analytic function to the data.

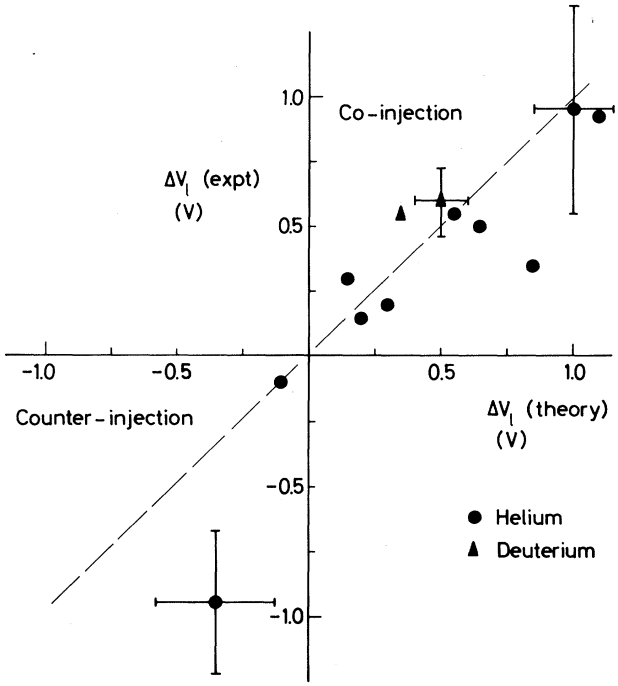

FIG. 3. Experimental and theoretical loop voltages (ΔV_l) caused by the beam current. Each point corresponds to the measurement of a T_e profile of which there are two during injection.

each magnetic surface. The local source rate of fast ions is obtained from a beam deposition code which includes finite-orbit-size effects. The radial profile of the beam-driven current density (j_{bd}) is then obtained from the fast ion current density (j_{fast}) using the expression given[8], which for this case reduces to

$$j_{bd}(r) = j_{\mathrm{fast}}(r)[1 - Z_b/Z_{\mathrm{eff}}]. \quad (1)$$

The second term on the right-hand side of Eq. (1) is the back electron current produced by momentum transfer from the fast ions. In DITE it approaches 50% of j_{fast}. Changes in the back electron current caused by plasma rotation, trapped electrons, and the neoclassical current contribute less than 10% to the beam-driven current and are neglected.

The electric field (E) is obtained as a function of time and radius from Ohm's law and Maxwell's equations,

$$\sigma E = j - j_{bd}, \quad \frac{1}{r}\frac{\partial}{\partial r}\left(r\frac{\partial E}{\partial r}\right) = \mu_0 \frac{\partial j}{\partial t}, \quad (2)$$

in which σ is the Spitzer[9] conductivity and j is the total current density. Equations (2) are solved numerically subject to the constraint that the total current is constant.

Figure 1 shows good agreement between experimental and theoretical loop voltages for both a low- and a high-density discharge. Also in Fig. 1 are theoretical curves with the beam-driven current omitted. For the low-density case [Fig. 1(a)], the reduction in loop voltage is entirely attributable to the beam-driven current, which replaces 33 kA of the original 80 kA of transformer-driven current. In the high-density case [Fig. 1(b)] the change in loop voltage is largely caused by changes in the T_e profile.

The change in loop voltage (ΔV_l) produced by the beam-driven current is compared with theory (excluding charge-exchange losses) in Fig. 3 for a range of densities, currents and Z_{eff} (Table I). The experimental ΔV_l is the difference between curves like (iii) and (i) of Fig. 1, while the theoretical ΔV_l is the difference between curves like (iii) and (ii). As expected, ΔV_l is negative for counterinjection, but its somewhat large magnitude may be caused by an underestimate of Z_{eff} during injection. The errors on the points are derived by following the errors on the measurements of T_e through the theoretical calculations of V_l.

An independent check on the calculated fast-ion distribution is provided by the simultaneous measurement of both the vertical field (B_V) required to maintain plasma equilibrium and the plasma diamagnetism (β_{loop}). For nonisotropic velocity distributions, B_V is given by Shafranov's formu-

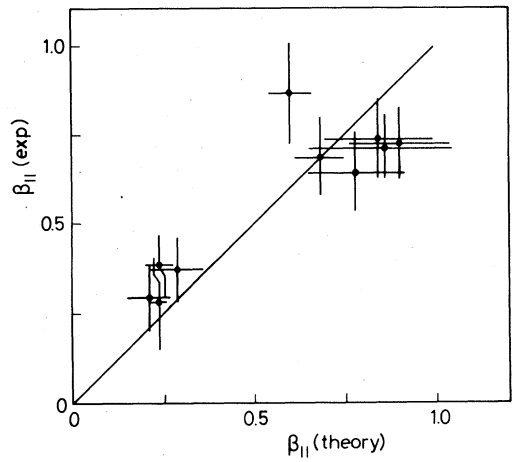

FIG. 4. Experimental and theoretical values of $\beta_{\parallel}$.

la[10]

$$B_V = (\mu_0 I_p/4\pi R) \times [\ln(8R/a) - \tfrac{3}{2} + \tfrac{1}{2} l_i + \tfrac{3}{4}\beta_\perp + \tfrac{3}{2}\beta_\parallel], \quad (3)$$

$$\beta_{\text{loop}} = \tfrac{3}{2}\beta_\perp, \quad (4)$$

where l_i is the inductance per unit length, and $\beta_{\parallel,\perp} = 4\sum m_i v^2{}_{i\parallel,\perp}/3\mu_0 R I_p{}^2$ with the sum over all plasma particles of mass m_i and velocity v_i. The inductance is obtained from the measured profiles, $T_e(r)$, assuming j is proportional to $T_e{}^{3/2}$. The background plasma pressure is assumed isotropic so that its contribution to $\beta_{\parallel,\perp}$ can be obtained from the measured profiles $T_e(r)$ and $n_e(r)$. Solution of Eqs. (3) and (4) then allows $\beta_{\parallel,\perp}$ for the fast ions to be obtained. The dominant term is $\beta_\parallel$ which is essentially the centrifugal pressure of the confined fast ions. In Fig. 4 this is compared with the predictions of the Fokker-Planck code. The good agreement constitutes an experimental check on a quantity similar to the total fast ion current and consequently on the neglect of charge exchange.

In summary, these experiments have demonstrated the existence of the beam-driven current in a tokamak. Its variation with plasma parameters agrees well with a kinetic theory which includes the fast ion current and the back electron current.

We thank our colleagues in the DITE and Injection Groups for their help, Dr. M. H. Hughes for supplying the field diffusion code, and Dr. D. R. Sweetman for his encouragement.

[1]T. Ohkawa, Nucl. Fusion 10, 185 (1970).

[2]D. F. H. Start, P. R. Collins, E. M. Jones, A. C. Riviere, and D. R. Sweetman, Phys. Rev. Lett. 40, 1497 (1978).

[3]J. W. M. Paul *et al.*, in *Proceedings of the Sixth International Conference on Plasma Physics and Controlled Nuclear Fusion Research, Berchtesgaden, West Germany, 1976* (International Atomic Energy Agency, Vienna, 1977), Vol. 2, p. 269.

[4]R. S. Hemsworth *et al.*, in *Proceedings of the Joint Varenna-Grenoble International Symposium on Heating in Toroidal Plasmas, Grenoble, France 3–7 July 1978,* edited by T. Consoli and P. Caldirola (Pergamon, Elmsford, N.Y., 1979), Vol. 1, p. 83.

[5]R. A. Hulse, D. E. Post, and D. R. Mikkelsen, Plasma Physics Laboratory, Princeton University Report No. PPPL-1633, 1980 (unpublished).

[6]R. D. Gill, K. B. Axon, J. W. M. Paul, and R. Prentice, Nucl. Fusion 19, 1003 (1979).

[7]C. E. Singer *et al.*, in *Proceedings of the Joint Varenna-Grenoble International Symposium on Heating in Toroidal Plasmas, Grenoble, France 3–7 July 1978,* edited by T. Consoli and P. Caldirola (Pergamon, Elmsford, N.Y., 1979), Vol. 1, p. 19.

[8]D. F. H. Start, J. G. Cordey, and E. M. Jones, Plasma Phys. 22, 303 (1980).

[9]L. Spitzer and R. Härm, Phys. Rev. 89, 977 (1953).

[10]V. S. Mukhovatov and V. D. Shafranov, Nucl. Fusion 11, 605 (1971); A. Mondelli and E. Ott, Phys. Fluids 17, 1017 (1974).